Localizing high-lying Rydberg wave packets with two-color laser fields

Seyedreza Larimian,[1] Christoph Lemell,[2,*] Vinzenz Stummer,[1] Ji-Wei Geng (耿基伟),[3] Stefan Roither,[1] Daniil Kartashov,[1] Li Zhang (张丽),[1] Mu-Xue Wang (王慕雪),[3] Qihuang Gong (龚旗煌),[3,4] Liang-You Peng (彭良友),[3,4,†] Shuhei Yoshida,[2] Joachim Burgdörfer,[2] Andrius Baltuška,[1] Markus Kitzler,[1] and Xinhua Xie (谢新华)[1,5,‡]

[1]*Photonics Institute, Technische Universität Wien, A-1040 Vienna, Austria, EU*
[2]*Institute for Theoretical Physics, Technische Universität Wien, A-1040 Vienna, Austria, EU*
[3]*State Key Laboratory for Mesoscopic Physics and Collaborative Innovation Center of Quantum Matter, School of Physics, Peking University, Beijing 100871, China*
[4]*Collaborative Innovation Center of Extreme Optics, Shanxi University, Taiyuan, Shanxi 030006, China*
[5]*Institute of Theoretical Chemistry, University of Vienna, A-1010 Vienna, Austria, EU*

We demonstrate control over the localization of high-lying Rydberg wave packets in argon atoms with phase-locked orthogonally polarized two-color laser fields. With a reaction microscope, we measure ionization signals of high-lying Rydberg states induced by a weak dc field and blackbody radiation as a function of the relative phase between the two-color fields. We find that the dc-field-ionization yield of high-lying Rydberg argon atoms oscillates with the relative two-color phase with a period of 2π while the photoionization signal by blackbody radiation shows a period of π. Accompanying simulations show that these observations are a clear signature of the asymmetric localization of electrons recaptured into very elongated (low angular momentum) high-lying Rydberg states after conclusion of the laser pulse. Our findings thus open an effective pathway to control the localization of high-lying Rydberg wave packets.

DOI: 10.1103/PhysRevA.96.021403

Highly excited Rydberg atoms and molecules, in comparison with ground-state atoms and molecules, have unique properties [1]. Such atoms and molecules can be exploited in the studies of quantum phenomena and the transition from the quantum to the classical worlds on a macroscopic length scale. They play an important role in chemistry and astrophysics and are also considered to be building blocks for future applications in quantum information, chemistry, and astrophysics [2]. Manipulating electrons in the ground and excited states of an atom or a molecule is of fundamental interest for physics and chemistry with a wide range of applications from high-harmonic generation [3] to the control of chemical reactions [4].

In a strong laser pulse, valence electrons of an atom or a molecule can be detached through tunneling or barrier-suppression ionization. After conclusion of the pulse, some of the released electrons may be recaptured by the ionic Coulomb field and populate highly excited Rydberg states (frustrated field ionization) [5]. Recently, we reported on the lifetime of such states measured by electron-ion coincidence spectroscopy [6]. It has been demonstrated that electronically excited states play an important role in strong-field phenomena including ionization and molecular dissociation [7,8], electron wave packet interference, and high-harmonic generation [9–12]. Many strong-field phenomena in atoms and molecules are governed by electronic dynamics that are sensitive not only to the laser intensity but also to the waveform of the laser field [13]. The latter can be controlled by varying the carrier-envelope phase of a few-cycle laser pulse or by

the superposition of phase-locked pulses with different colors [13,14].

In this Rapid Communication we report on the control of the formation of spatially localized high-lying Rydberg wave packets by waveform controlled orthogonally polarized two-color (OTC) laser fields in argon atoms. With the help of semiclassical electron-trajectory simulations, we analyze the experimental observation and identify the underlying mechanism. In the present experiment we exploit the relative phase of OTC laser fields to achieve temporal and spatial shaping of the waveform of the laser field. Previously, OTC fields were proposed and successfully applied to control electron rescattering and interference [11,15–17], to image atomic wave functions based on high-harmonic generation [18], and to control electron emission and correlation in single and double ionization of atoms [19]. Since controlling the waveform of an OTC laser field provides the capability of manipulating electron trajectories in time and space, one may expect to achieve control over the formation of high-lying Rydberg states [7,20–23].

In our experiment (Fig. 1), we use a reaction microscope to perform coincidence measurements of electrons and ions separated by the interaction of argon atoms with the laser and the weak dc fields [24]. The ionization signal of Rydberg states can be well distinguished from that of the prompt laser-induced strong-field ionization and retains a very high signal-to-noise ratio. Details of the experimental setup can be found in our previous publications [10,25]. Measurements were done with OTC laser fields formed by the superposition of a fundamental pulse with a center wavelength of 800 nm and its second harmonic with pulse durations (full width at half maximum intensity) of 46 and 48 fs, respectively. Temporal overlap of the two pulses was ensured by compensating their different group velocities with calcite plates and a pair of fused silica wedges. The electric field of the OTC pulses can

*lemell@concord.itp.tuwien.ac.at
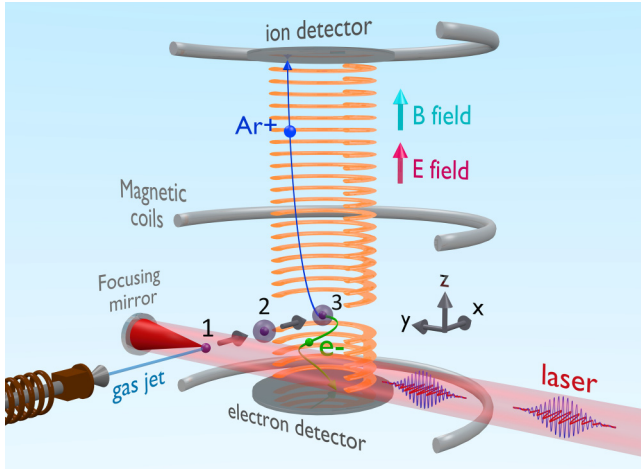†liangyou.peng@pku.edu.cn
‡xinhua.xie@tuwien.ac.at

FIG. 1. Schematic view of the experiment. An electron from an argon atom released by the field of an OTC laser pulse may be recaptured into a high-lying Rydberg state by frustrated field ionization. The Rydberg atom in turn is subsequently ionized either by the weak dc field in the target region or by photoionization by blackbody radiation.

be written as $\vec{F}(t,\Delta\varphi) = f_x(t)\cos(\omega t)\hat{\mathbf{e}}_x + f_z(t)\cos(2\omega t + \Delta\varphi)\hat{\mathbf{e}}_z$, with $\Delta\varphi$ the relative phase of the two colors and $f_{x,z}$ the pulse envelopes. The waveform of the OTC pulse can be precisely controlled on a subcycle time scale by adjusting the position of one of the wedges. The peak laser intensity was about 6×10^{13} W/cm^2 (peak electric field on the order of 2×10^8 V/cm) for each color. A weak homogeneous dc field of 1.5 V/cm was applied in the time-of-flight (TOF) spectrometer [along the polarization direction ($\hat{z}$) of the 400-nm pulse] to accelerate charged particles towards the detectors. This field also induces field ionization of high-lying Rydberg states populated during the strong-field–atom interaction [6]. A homogeneous magnetic field of 12 G was applied to ensure 4π detection of electrons with velocities $v < 1.93$ a.u. ($E_{\text{kin}} \lesssim 50$ eV). With our reaction microscope it is possible to observe electron-ion coincidences both from direct ionization events during the duration of the laser pulse and from delayed emission up to 23 μs after the pulse.

The strong laser field not only induces tunneling ionization of argon atoms but may also excite them to long-lived high-lying Rydberg states through electron recapture [6,20,22]. These high-lying Rydberg states can be ionized by a very weak dc field through over-the-barrier or tunneling ionization [26] or through photoionization by photons absorbed from blackbody radiation (BBR) [27]. A typical photoelectron photoion coincidence distribution for argon interacting with an intense OTC field is shown in Fig. 2(a). The delayed ionization signal from high-lying Rydberg atoms appears along the diagonal and can be easily separated from the prompt strong-field-ionization signal. The final momentum of the ions and electrons from the strong-field ionization is determined by the vector potential of the external laser field at the ionization time. In the case of an OTC laser field the cycle waveform changes periodically with the relative phase between the two laser components [19], leading to a periodic modulation of the momentum distribution of the argon ions
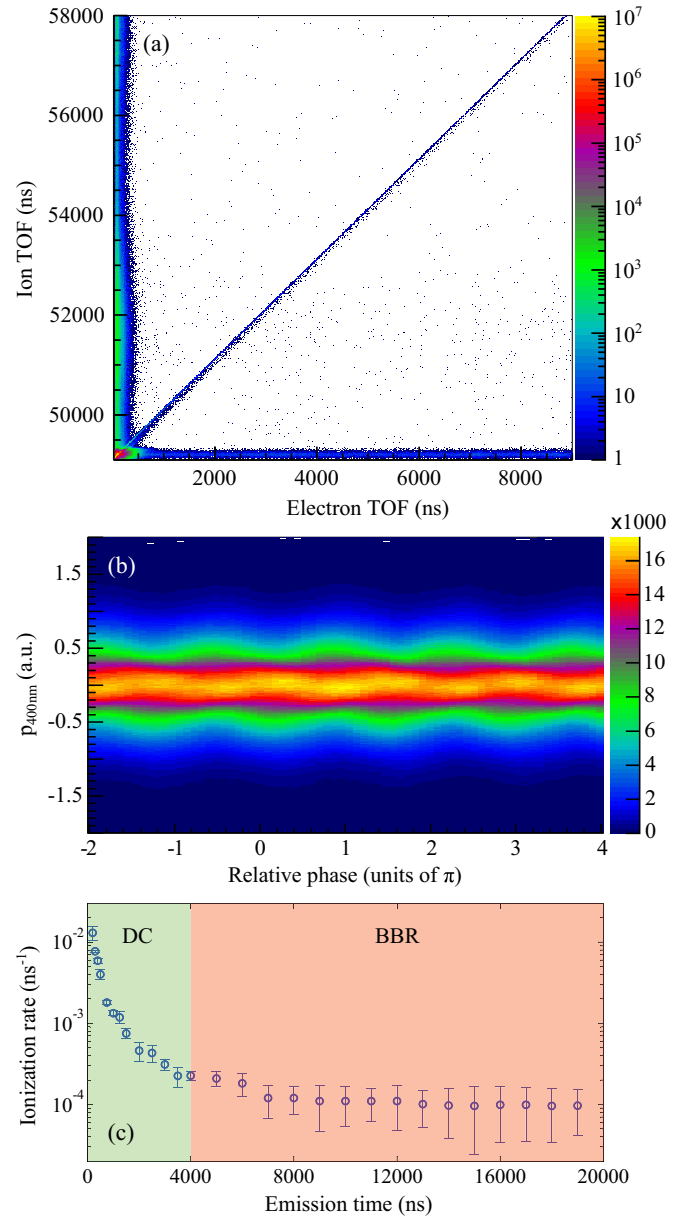

FIG. 2. (a) Photoelectron-photoion-coincidence distribution for argon. The peak laser field strength of each color is 2×10^8 V/cm and the spectrometer dc-field strength is 1.5 V/cm. (b) Measured momentum distribution of strong-field ionized Ar$^+$ along the polarization direction ($\hat{z}$) of the 400-nm pulse as a function of the relative phase $\Delta\varphi$ between the two color fields. (c) Ionization rate of Rydberg states induced by the dc field and blackbody radiation.

with the relative phase. In Fig. 2(b) the measured momentum distribution of Ar$^+$ from the strong-field-induced ionization along the polarization axis of the 400-nm pulse is shown as a function of the relative phase. The clear periodic dependence of the momentum distribution on the relative phase indicates that a precise control of the cycle shape of the OTC field with the relative phase was achieved in the experiments.

From the correlated TOF signal between electrons and argon ions the emission time of the electrons from Rydberg atoms and the corresponding ionization rate $\Gamma = -d\ln[I(\tau)]/d\tau$ [with $I(\tau)$ the ionization yield and τ the

emission time of the electron after the conclusion of the laser pulse] are extracted [Fig. 2(c)]. The rate decreases from about $\Gamma \approx 0.01$ ns^{-1} at $\tau = 200$ ns to about 2×10^{-4} ns^{-1} at $\tau = 4\,\mu$s [green shaded area in Fig. 2(c)]. Electron emission in this time range is dominated by field emission due to the weak dc extraction field applied along the spectrometer direction. The rapidly decaying ($\lesssim 1\,\mu$s) component of the signal results from dc-field ionization of Rydberg states very close to the continuum threshold and well above the potential barrier (diabatic field-ionization threshold $F_{dc} = 1/9n_F^4$ yielding $n_F \simeq 140$). For emission times longer than $6\,\mu$s photoelectrons ionized by BBR at room temperature with a mean photon energy of about 0.026 eV [28] from Rydberg states with $n > n_{BBR} \simeq 23$ are detected. The ionization rate becomes nearly constant with a value of $\Gamma \approx 1 \times 10^{-4}$ ns^{-1}, which is in good agreement with the simulated photon-ionization rate by BBR [6].

To study the formation of high-lying Rydberg atoms in the presence of OTC fields, we have performed semiclassical electron transport simulations [6] that have been adapted to the present experimental conditions. Using the coordinate system of Fig. 1, two orthogonally polarized 400- and 800-nm pulses with pulse durations and peak intensities from the experiment interact with the single active electrons of Ar atoms represented by a Hartree-Fock potential $V_{HF}(r)$ [29]. For the ionization rate and Gaussian momentum distribution perpendicular to the field direction at the tunnel exit we use the results of Delone and Krainov for circularly polarized light with $\sigma_{p_\perp}^2 = F/2\sqrt{2I_p}$, with I_p the binding energy and $p_\parallel = 0$ [30]. Note that all results discussed below are remarkably insensitive to the particular choices of pulse durations, intensity envelope, or momentum distributions at the tunnel exit. The intensity distribution of the laser focus [31] and the weak dc field in the interaction region are taken into account. After conclusion of the pulse the Kepler orbits of the released electrons are analyzed. For electrons with total energy $E > 0$ the asymptotic momentum vector $\vec{p}$ is calculated [32], while for recaptured electrons with negative energies [$E = p^2/2 + V_{HF}(r) < 0$], we classify their orbits according to their angular momentum and Runge-Lenz vectors $\vec{L}$ and $\vec{A}$, respectively [Figs. 3(a) and 3(b)].

The starting point of our analysis is the inversion symmetry of the free atom and the π periodicity of the laser intensity $|\vec{F}(\Delta\varphi)|^2 = |\vec{F}(\Delta\varphi + \pi)|^2$. Therefore, all processes that do not depend on the direction of the dc field (including the formation of high-lying Rydberg states) will feature such a periodicity. This is indeed observed in our simulation when counting the number of electrons with negative final energy but larger than $\hbar\omega_{BBR}$ photons ($n > n_{BBR}$) [red line in Fig. 3(d)]. As blackbody radiation is isotropic, the measured yield of postpulse photoionized Rydberg atoms is directly proportional to the number of available highly excited atoms and consequently exhibits the same π periodicity [blue circles with error bars in Fig. 3(d)].

The situation is different for the postpulse dc-field ionization where the weak extraction field present in the interaction region breaks the inversion symmetry of the system. Only Rydberg orbits with hydrogenic principal quantum number $n \gtrsim 140$ may overcome the potential saddle in the $-z$ direction (Fig. 4). For these high-lying Rydberg electrons we find a very narrow distribution of $|\vec{A}|$ close to 1, indicating cigar-shaped
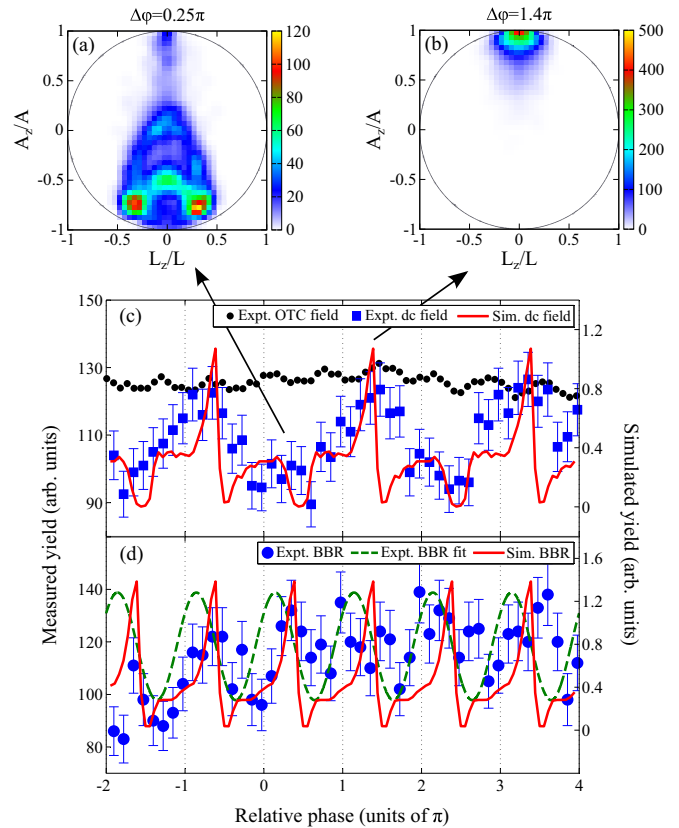

FIG. 3. Runge-Lenz vector A_z/A vs angular momentum component L_z/L for relative phases (a) $\Delta\varphi = 0.25\pi$ and (b) $\Delta\varphi = 1.4\pi$. In the latter case virtually all Rydberg orbits point towards the potential saddle (Fig. 4). (c) Normalized experimental strong-field-ionization yield (black dots) and dc-field-ionization yield (blue squares with error bars) from high-lying Rydberg states as a function of the two-color relative phase. The simulated yield (red line) reproduces the 2π periodicity and the local maximum around $\Delta\varphi \approx 2m\pi$ ($m = -1, 0, 1, 2$). (d) Normalized BBR photoionization yield (blue circles with error bars) with a sinusoidal fitting curve (green dashed line) and simulated population of Rydberg states with $n > n_{BBR}$ (red line). In all panels the absolute value of the two-color relative phase has been determined by matching experimental and simulated maxima and minima in (c).

very elongated orbits (for representative examples see Fig. 4). This coincides with small angular momentum values $L < 10$ corresponding to a normalized value of $L/L_{max} \ll 1$. Such orbits feature a large dipole moment that slowly precesses about the electric field F_{dc}. From the shape of the orbits and the potential landscape it appears obvious that redshifted "downhill" orbits pointing towards the potential barrier formed by the Coulomb and static dc fields (Fig. 4) will more easily overcome the potential barrier than blueshifted "uphill" orbits [6]. Consequently, as $\vec{A}$ points towards the distance of closest approach of the electron to the core we expect orbits with A_z/A close to $+1$ to have the largest escape probability [Fig. 3(b)]. The number of dc-field-ionized electrons can now be estimated by counting orbits fulfilling the above-the-barrier condition for
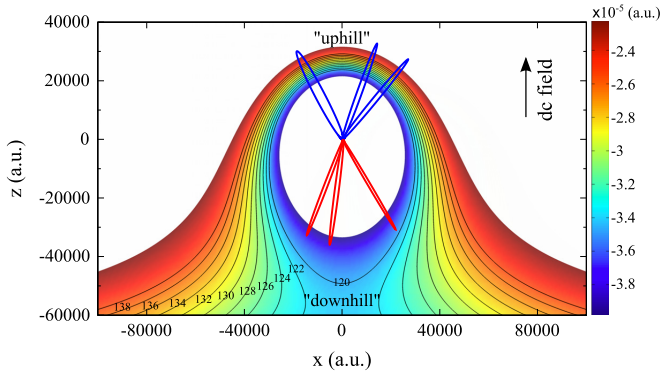
FIG. 4. Rydberg orbits in the combined Coulomb and weak dc fields ($F_{dc} = 1.5$ V/cm). The contour lines denote the energy levels of hydrogenic Rydberg states with their corresponding principal quantum numbers. The red and blue ellipses represent orbitals of redshifted and blueshifted Rydberg-Stark states, respectively.

the barrier height V_b [33],

$$V_b \approx -\sqrt{2(1 + A_z)F_{dc}} < -\frac{1}{2n^2} - \frac{3F_{dc}n^2 A_z}{2}, \quad (1)$$

where the second term on the right-hand side is the Stark correction of the hydrogenic energy in the dc field [33]. We compare the number of dc-field-ionized Rydberg atoms [Fig. 3(c)] with the experimental dc-field-ionization yield determined by integrating the signal over emission times in the interval between 100 ns and 4 μs after the laser pulse conclusion. This yield [blue squares with error bars in Fig. 3(c)] exhibits a clear 2π periodicity that is well reproduced by our simulation (red line), allowing for the determination of the relative ω-2ω phase in the experiment. It is important to note that this 2π periodicity is related neither to the strong-field-ionization yield (black dots) [Fig. 3(c)], which is almost constant for all relative phases, nor to the (simulated) electron recapture rate, which oscillates with π periodicity. The latter is directly related to the $\Delta\varphi$ oscillations of the photoionization yield by BBR for electron emission times longer than 4 μs [Fig. 3(d)]. The origin of the observed different periodicities lies in the localization of the Rydberg wave packet [Figs. 3(a) and 3(b)] due to the controlled driving of the photoelectron by the OTC field in combination with

the broken inversion symmetry due to the presence of the weak dc field. The maximum of the yield [Fig. 3(c)] is correlated with the strong localization of orbits in the *A*-*L* plane corresponding to downhill orientation [Fig. 3(b)], while minima are associated with a broad distribution on the uphill side [Fig. 3(a)]. The agreement between the simulated and measured emission yields, which is largely independent of the chosen parameters, lends credibility to the semiclassical simulation and points in turn to a large degree of spatial localization of states in laser-atom interactions by controlling the waveform of the exciting laser pulse.

In conclusion, we have presented a joint experimental and theoretical study on highly excited Rydberg states created during the interaction of argon atoms with waveform controlled OTC laser fields. The ionization yields due to weak-dc-field ionization and BBR photoionization could be measured separately as a function of the relative phase between the two colors. We found different oscillation periods of 2π and π, respectively. The measurements and analysis of trajectories calculated in a semiclassical simulation suggest that Rydberg electrons recaptured by the ion after conclusion of the pulse can be preferentially steered and aligned along the 2ω laser field polarization direction by the shape of the OTC waveform. We have demonstrated this steering in our experiment by manipulating the relative phase between the two colors. For specific two-color phases, Rydberg wave packets with energies above the potential barrier are predominantly localized on the downhill side of the atom. The ionization yield of such electrons induced by a weak dc field is significantly increased and shows a modulation with a period of 2π. The present study opens an effective way to control the population and the localization of high-lying Rydberg wave packets and may find potential applications in the manipulation of interacting Rydberg ensembles, Rydberg molecules, and chemistry.

[1] T. F. Gallagher, *Rydberg Atoms* (Cambridge University Press, Cambridge, 2005), Vol. 3.

[2] M. Saffman, T. G. Walker, and K. Molmer, Rev. Mod. Phys. **82**, 2313 (2010); F. Merkt, Annu. Rev. Phys. Chem. **48**, 675 (1997); Yu. N. Gnedin, A. A. Mihajlov, Lj. M. Ignjatović, N. M. Sakan, V. A. Srećković, M. Yu. Zakharov, N. N. Bezuglov, and A. N. Klycharev, New Astron. Rev. **53**, 259 (2009).

[3] C. Winterfeldt, C. Spielmann, and G. Gerber, Rev. Mod. Phys. **80**, 117 (2008).

[4] R. E. Carley, E. Heesel, and H. H. Fielding, Chem. Soc. Rev. **34**, 949 (2005).

[5] F. Krausz and M. Ivanov, Rev. Mod. Phys. **81**, 163 (2009).

[6] S. Larimian, S. Erattupuzha, C. Lemell, S. Yoshida, S. Nagele, R. Maurer, A. Baltuska, J. Burgdörfer, M. Kitzler, and X. Xie, Phys. Rev. A **94**, 033401 (2016).

[7] B. Wolter, C. Lemell, M. Baudisch, M. G. Pullen, X.-M. Tong, M. Hemmer, A. Senftleben, C. D. Schröter, J. Ullrich, R. Moshammer, J. Biegert, and J. Burgdörfer, Phys. Rev. A **90**, 063424 (2014); Q. Li, X.-M. Tong, T. Morishita, C. Jin, H. Wei, and C. D. Lin, J. Phys. B **47**, 204019 (2014); H. Liu, Y. Liu, L. Fu, G. Xin, D. Ye, J. Liu, X. T. He, Y. Yang, X. Liu, Y. Deng, C. Wu, and Q. Gong, Phys. Rev. Lett. **109**, 093001 (2012).

[8] R. Minns, D. Lazenby, F. Hall, N. Jones, R. Patel, and H. Fielding, Mol. Phys. **112**, 1808 (2014).

[9] M. Chini, X. Wang, Y. Cheng, H. Wang, Y. Wu, E. Cunningham, P.-C. Li, J. Heslar, D. A. Telnov, S.-I. Chu, and Z. Chang, Nat. Photon. **8**, 437 (2014).

[10] X. Xie, S. Roither, D. Kartashov, E. Persson, D. G. Arbo, L. Zhang, S. Gräfe, M. S. Schöffler, J. Burgdörfer, A. Baltuska, and M. Kitzler, Phys. Rev. Lett. **108**, 193004 (2012).

[11] X. Xie, Phys. Rev. Lett. **114**, 173003 (2015); Y. Deng and X. Xie, Phys. Rev. A **91**, 043414 (2015).

[12] D. G. Arbo, S. Nagele, X.-M. Tong, X. Xie, M. Kitzler, and J. Burgdörfer, Phys. Rev. A **89**, 043414 (2014).

[13] A. Baltuska, T. Udem, M. Uiberacker, M. Hentschel, E. Goulielmakis, C. Gohle, R. Holzwarth, V. S. Yakovlev, A. Scrinzi, T. W. Hänsch, and F. Krausz, Nature (London) **421**, 611 (2003).

[14] H.-S. Chan, Z.-M. Hsieh, W.-H. Liang, A. H. Kung, C.-K. Lee, C.-J. Lai, R.-P. Pan, and L.-H. Peng, Science **331**, 1165 (2011).

[15] M. Kitzler and M. Lezius, Phys. Rev. Lett. **95**, 253001 (2005); M. Kitzler, X. Xie, A. Scrinzi, and A. Baltuska, Phys. Rev. A **76**, 011801 (2007).

[16] M. Richter, M. Kunitski, M. Schöffler, T. Jahnke, L. P. H. Schmidt, M. Li, Y. Liu, and R. Dörner, Phys. Rev. Lett. **114**, 143001 (2015).

[17] J.-W. Geng, W.-H. Xiong, X.-R. Xiao, L.-Y. Peng, and Q. Gong, Phys. Rev. Lett. **115**, 193001 (2015).

[18] M. Kitzler, X. Xie, S. Roither, A. Scrinzi, and A. Baltuska, New J. Phys. **10**, 025029 (2008); D. Shafir, Y. Mairesse, D. Villeneuve, P. Corkum, and N. Dudovich, Nat. Phys. **5**, 412 (2009).

[19] L. Zhang, X. Xie, S. Roither, Y. Zhou, P. Lu, D. Kartashov, M. Schöffler, D. Shafir, P. B. Corkum, A. Baltuska, A. Staudte, and M. Kitzler, Phys. Rev. Lett. **112**, 193002 (2014); Y. Zhou, C. Huang, A. Tong, Q. Liao, and P. Lu, Opt. Express **19**, 2301 (2011); L. Zhang, X. Xie, S. Roither, D. Kartashov, Y. L. Wang, C. L. Wang, M. Schöffler, D. Shafir, P. B. Corkum, A. Baltuška, I. Ivanov, A. Kheifets, X. J. Liu, A. Staudté, and M. Kitzler, Phys. Rev. A **90**, 061401(R) (2014).

[20] T. Nubbemeyer, K. Gorling, A. Saenz, U. Eichmann, and W. Sandner, Phys. Rev. Lett. **101**, 233001 (2008); U. Eichmann, T. Nubbemeyer, H. Rottke, and W. Sandner, Nature (London) **461**, 1261 (2009); U. Eichmann, A. Saenz, S. Eilzer, T. Nubbemeyer, and W. Sandner, Phys. Rev. Lett. **110**, 203002 (2013).

[21] A. S. Landsman, A. N. Pfeiffer, C. Hofmann, M. Smolarski, C. Cirelli, and U. Keller, New J. Phys. **15**, 013001 (2013).

[22] E. Diesen, U. Saalmann, M. Richter, M. Kunitski, R. Dörner, and J. M. Rost, Phys. Rev. Lett. **116**, 143006 (2016).

[23] J. B. Williams, U. Saalmann, F. Trinter, M. S. Schöffler, M. Weller, P. Burzynski, C. Goihl, K. Henrichs, C. Janke, B. Griffin, G. Kastirke, J. Neff, M. Pitzer, M. Waitz, Y. Yang, G. Schiwietz, S. Zeller, T. Jahnke, and R. Dörner, J. Phys. B **50**, 034002 (2017).

[24] J. Ullrich, R. Moshammer, A. Dorn, R. Dörner, L. P. H. Schmidt, and H. Schmidt-Böcking, Rep. Prog. Phys. **66**, 1463 (2003); R. Dörner, V. Mergel, O. Jagutzki, J. U. L. Spielberger, R. Moshammer, and H. Schmidt-Böcking, Phys. Rep. **330**, 95 (2000).

[25] X. Xie, K. Doblhoff-Dier, S. Roither, M. S. Schöffler, D. Kartashov, H. Xu, T. Rathje, G. G. Paulus, A. Baltuska, S. Gräfe, and M. Kitzler, Phys. Rev. Lett. **109**, 243001 (2012).

[26] T. Morishita and C. D. Lin, Phys. Rev. A **87**, 063405 (2013).

[27] T. F. Gallagher and W. E. Cooke, Phys. Rev. Lett. **42**, 835 (1979).

[28] W. P. Spencer, A. G. Vaidyanathan, D. Kleppner, and T. W. Ducas, Phys. Rev. A **26**, 1490 (1982); I. I. Beterov, D. B. Tretyakov, I. I. Ryabtsev, V. M. Entin, A. Ekers, and N. N. Bezuglov, New J. Phys. **11**, 013052 (2009).

[29] C. Froese Fischer, Comput. Phys. Commun. **43**, 355 (1987).

[30] N. B. Delone and V. P. Krainov, J. Opt. Soc. Am. B **8**, 1207 (1991).

[31] S. Augst, D. D. Meyerhofer, D. Strickland, and S. L. Chin, J. Opt. Soc. Am. B **8**, 858 (1991).

[32] N. I. Shvetsov-Shilovski, D. Dimitrovski, and L. B. Madsen, Phys. Rev. A **85**, 023428 (2012).

[33] C. O. Reinhold, S. Yoshida, and F. B. Dunning, J. Chem. Phys. **134**, 174305 (2011).